Supplementary Information for

“Time-correlated electron and photon counting microscopy”

Sotatsu Yanagimoto[1], Naoki Yamamoto[1], Tatsuro Yuge[2], Hikaru Saito[1,3], Keiichirou Akiba[1,4*],

Takumi Sannomiya[1 †]

[1] Department of Materials Science and Engineering, School of Materials and Chemical Technology, Tokyo Institute of Technology, 4259 Nagatsuta, Midoriku, Yokohama, 226-8503, Japan

[2]Department of Physics, Shizuoka University, Shizuoka, Shizuoka, 422-8529, Japan

[3] Department of Integrated Materials, Institute for Materials Chemistry and Engineering, Kyushu University, 6-1 Kasugakoen, Kasuga, Fukuoka 816-8580, Japan

[4] Takasaki Institute for Advanced Quantum Science, National Institutes for Quantum Science and Technology, 1233 Watanuki, Takasaki, Gunma, 370-1292, Japan

[*] akiba.keiichiro@qst.go.jp

[†] sannomiya.t.aa@m.titech.ac.jp

Supplementary Note 1:

DERIVATION OF ASYMMETRIC CROSS-CORRELATION FUNCTION $g^{(2)}_{AB}(\tau)$

To derive the asymmetric correlation function, we consider that the target material A contains enough luminescent centers. As previously demonstrated and calculated, when a single incident electron excites multiple luminescent centers of the material simultaneously, a photon bunching phenomenon occurs[1]. The 2nd order autocorrelation function of the emitted photons from material A, $g^{(2)}_{A(auto)}(\tau)$, obtained from the conventional CL-HBT experiment, has a symmetric functional form[1,2]. Let us now consider an event in which a single incident electron simultaneously excites two materials A and B, both of which contain a large number of emission centers. In this case, the 2nd order cross-correlation function $g^{(2)}_{AB}(\tau)$, which is the time correlation between the photons emitted from A and B, shows "bunching" and gives asymmetric electron-photon correlation functions. Now we assume a situation where the electron beam current is weak enough that an excitation process of one incident electron has no influence on the next electron excitation.

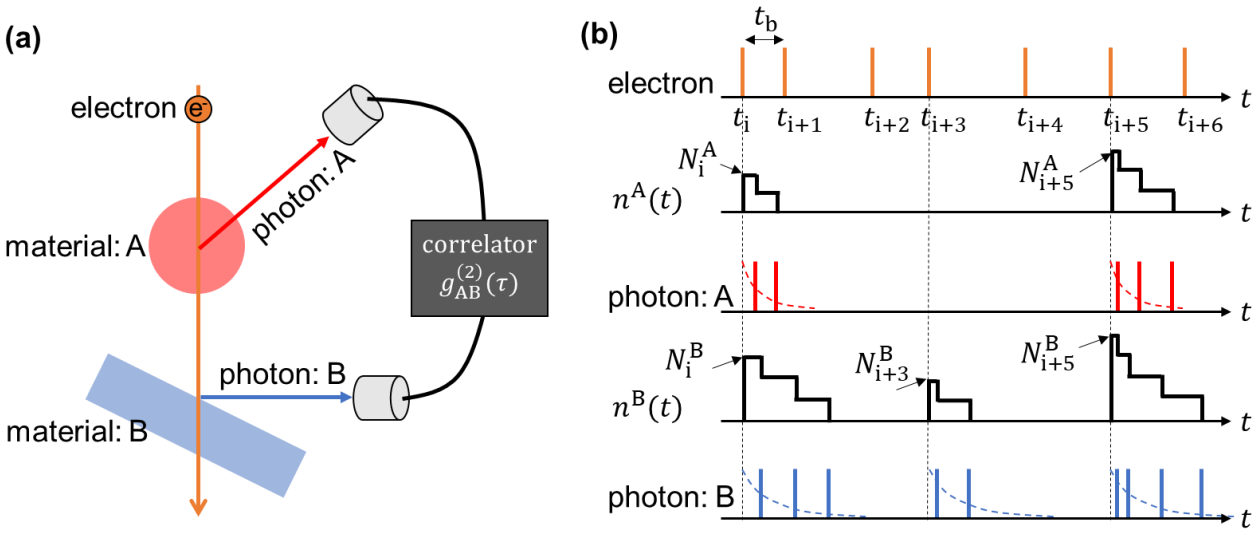

Fig. S1 Concept of the electron-photon correlation. (a) Schematic diagram of electron-photon correlation measurement. A single fast electron excites materials A and B almost simultaneously, and their time correlations are measured. (b) Classical picture of the relation among electron incidence, number of excited emission centers $n^{A(B)}(t)$ and photon emission from the materials A and B.

For the electron beam current I_b, the average time interval t_b between consecutive electron incidences is given by $t_b = (I_b/e)^{-1}$. Using the number of events N_e of fast electrons incident onto the sample during the measurement time T, the following equation holds:

$$\lim_{T\to\infty} \frac{N_e}{T} = \frac{1}{t_b}. \tag{S1}$$

First, we consider the excitation and relaxation processes of material A. Let $G^A(t)$ be a function that expresses the excitation of material A. It can be written as

$$G^A(t) = \sum_{i=1}^{N_e} N_i^A \delta(t - t_i), \tag{S2}$$

where $N_{\mathrm{i}}^{\mathrm{A}}$ is the number of emission centers that are simultaneously excited at time t_{i}. Using the average excitation number of emission centers per electron $N_{\mathrm{ex}}^{\mathrm{A}}$, the average excitation rate G^{A} is given by

$$G^{\mathrm{A}} = \langle G^{\mathrm{A}}(t) \rangle = \frac{N_{\mathrm{ex}}^{\mathrm{A}}}{t_{\mathrm{b}}}. \tag{S3}$$

If the number of centers at the excited state at time t is $n^{\mathrm{A}}(t)$, the rate equation is expressed as

$$\frac{dn^{\mathrm{A}}(t)}{dt} = G^{\mathrm{A}}(t) - \gamma^{\mathrm{A}} n^{\mathrm{A}}(t), \tag{S4}$$

where $\gamma^{\mathrm{A}} = \gamma_{\mathrm{r}}^{\mathrm{A}} + \gamma_{\mathrm{nr}}^{\mathrm{A}}$ is the total decay rate considering the radiative and non-radiative decay paths. Between the time t_{i} and $t_{\mathrm{i+1}}$, no excitation occurs, thus the rate equation from a single excitation event can be described as

$$\frac{dn^{\mathrm{A}}(t)}{dt} = -\gamma^{\mathrm{A}} n^{\mathrm{A}}(t), \tag{S5}$$

and the solution of the single process with the initial condition that $n_{\mathrm{i}}^{\mathrm{A}}(0) = N_{\mathrm{i}}^{\mathrm{A}}$ at $t = t_{\mathrm{i}} = 0$, is given by

$$n^{\mathrm{A}}(t) = N_{\mathrm{i}}^{\mathrm{A}} e^{-\gamma^{\mathrm{A}} t}. \tag{S6}$$

This situation is schematically illustrated in Fig. S1. The single excitation-emission process is repeated for each randomly incident electron. When N_{e} electron incidence events occur over a sufficiently long-time range, the total number $n^{\mathrm{A}}(t)$ is expressed by

$$n^{\mathrm{A}}(t) = \sum_{\mathrm{i}=1}^{N_{\mathrm{e}}} N_{\mathrm{i}}^{\mathrm{A}}\, e^{-\gamma^{\mathrm{A}}(t-t_{\mathrm{i}})} \theta(t - t_{\mathrm{i}}), \tag{S7}$$

where $\theta(t-t_{\mathrm{i}})$ is a step function, i.e., $\theta(t-t_{\mathrm{i}})=1$ for $t \geq t_{\mathrm{i}}$ and 0 for $t<t_{\mathrm{i}}$. In the same manner, the number of excited centers in material B, $n^{\mathrm{B}}(t)$, is described as

$$n^{\mathrm{B}}(t)=\sum_{\mathrm{i}=1}^{N_{\mathrm{e}}} N_{\mathrm{i}}^{\mathrm{B}}\, e^{-\gamma^{\mathrm{B}}(t-t_{\mathrm{i}})}\theta(t-t_{\mathrm{i}}). \tag{S8}$$

Since the photon emission intensity from the sample A (B) is proportional to $n^{\mathrm{A(B)}}(t)$, the 2nd order cross-correlation function $g_{\mathrm{AB}}^{(2)}(\tau)$ at detection time delay τ for photons from A and B is defined as

$$g_{\mathrm{AB}}^{(2)}(\tau)=\frac{\langle I^{\mathrm{A}}(t+\tau)\, I^{\mathrm{B}}(t)\rangle}{\langle I^{\mathrm{A}}(t+\tau)\rangle\langle\, I^{\mathrm{B}}(t)\rangle}=\frac{\langle n^{\mathrm{A}}(t+\tau)\, n^{\mathrm{B}}(t)\rangle}{\langle n^{\mathrm{A}}(t+\tau)\rangle\langle\, n^{\mathrm{B}}(t)\rangle}. \tag{S9}$$

According to the ergodic theorems, $\langle n^{\mathrm{A(B)}}(t)\rangle$ can be calculated as the time average of $n^{\mathrm{A(B)}}(t)$:

$$\langle n^{\mathrm{A}}(t)\rangle=\lim_{T\to\infty}\frac{1}{T}\int_0^T\sum_{\mathrm{i}=1}^{N_{\mathrm{e}}} N_{\mathrm{i}}^{\mathrm{A}}e^{-\gamma^{\mathrm{A}}(t-t_{\mathrm{i}})}\,\theta(t-t_{\mathrm{i}})dt=\lim_{T\to\infty}\frac{1}{T}\sum_{\mathrm{i}=1}^{N_{\mathrm{e}}} N_{\mathrm{i}}^{\mathrm{A}}\int_{-t_{\mathrm{i}}}^{T-t_{\mathrm{i}}} e^{-\gamma^{\mathrm{A}}t}\,\theta(t)dt$$

$$=\lim_{T\to\infty}\frac{1}{T}\sum_{\mathrm{i}=1}^{N_{\mathrm{e}}} N_{\mathrm{i}}^{\mathrm{A}}\,\frac{1}{\gamma^{\mathrm{A}}}=\frac{N_{\mathrm{ex}}^{\mathrm{A}}}{\gamma^{\mathrm{A}}t_{\mathrm{b}}}, \tag{S10}$$

$$\langle n^{\mathrm{B}}(t)\rangle=\frac{N_{\mathrm{ex}}^{\mathrm{B}}}{\gamma^{\mathrm{B}}t_{\mathrm{b}}}. \tag{S11}$$

The inverse Fourier transform of $n^{\mathrm{A(B)}}(t)$ is defined as

$$n^{\mathrm{A(B)}}(t)=\frac{1}{2\pi}\int_{-\infty}^{\infty} n_{\omega}^{\mathrm{A(B)}}(\omega)e^{-i\omega t}d\omega\,. \tag{S12}$$

Using Wiener-Khinchin theorem, the correlation function $\langle n^{\mathrm{A}}(t+\tau)\, n^{\mathrm{B}}(t)\rangle$ is calculated as follows

$$\langle n^{\mathrm{A}}(t+\tau)\, n^{\mathrm{B}}(t)\rangle=\lim_{T\to\infty}\frac{1}{T}\int_{-T}^{T} n^{\mathrm{A}}(t+\tau)n^{\mathrm{B}}(t)dt$$

$$=\lim_{T\to\infty}\frac{1}{T}\int_{-T}^{T}dt\,\frac{1}{2\pi}\int_{-\infty}^{\infty} n_{\omega}^{\mathrm{B}}(\omega')e^{i\omega' t}d\omega'\;\frac{1}{2\pi}\int_{-\infty}^{\infty} n_{\omega}^{\mathrm{A}}(\omega)e^{i\omega(t+\tau)}d\omega$$

$$= \lim_{T\to\infty} \frac{1}{T}\int_{-T}^{T} dt\ \frac{1}{2\pi}\int_{-\infty}^{\infty} n_{\omega}^{\mathrm{B}}(-\omega')e^{-i\omega' t}d\omega'\ \frac{1}{2\pi}\int_{-\infty}^{\infty} n_{\omega}^{\mathrm{A}}(\omega)e^{i\omega(t+\tau)}d\omega$$

$$= \lim_{T\to\infty} \frac{1}{T}\int_{-\infty}^{\infty} d\omega' \frac{1}{2\pi}\int_{-\infty}^{\infty} d\omega\ n_{\omega}^{\mathrm{A}}(\omega)\ n_{\omega}^{\mathrm{B}}(-\omega')\ e^{i\omega\tau}\left[\frac{1}{2\pi}\int_{-T}^{T} dt\ e^{i(\omega-\omega')t}\right]$$

$$= \lim_{T\to\infty} \frac{1}{2\pi}\int_{-\infty}^{\infty} \frac{1}{T} n_{\omega}^{\mathrm{A}}(\omega) n_{\omega}^{\mathrm{B}}(-\omega)e^{i\omega\tau}d\omega\,. \tag{S13}$$

Furthermore, considering $n_{\omega}^{\mathrm{A(B)}}(\omega)$ the Fourier transform of $n^{\mathrm{A(B)}}(t)$ defined as

$$n_{\omega}^{\mathrm{A}}(\omega) = \int_{-\infty}^{\infty} n^{\mathrm{A}}(t)e^{-i\omega t}dt = \frac{1}{\gamma^{\mathrm{A}} + i\omega}\sum_{\mathrm{k}=1}^{N_{\mathrm{e}}} N_{\mathrm{k}}^{\mathrm{A}} e^{i\omega t_{\mathrm{k}}} \quad , \tag{S14}$$

$$n_{\omega}^{\mathrm{B}}(-\omega) = \frac{1}{\gamma^{\mathrm{B}} - i\omega}\sum_{\mathrm{k}=1}^{N_{\mathrm{e}}} N_{\mathrm{k}}^{\mathrm{B}} e^{-i\omega t_{\mathrm{k}}} \quad . \tag{S15}$$

Inserting (S14) and (S15) to (S13), and after some algebra, we obtain

$$\langle n^{\mathrm{A}}(t+\tau)n^{\mathrm{B}}(t)\rangle = \frac{\xi^{\mathrm{AB}} N_{\mathrm{ex}}^{\mathrm{A}} N_{\mathrm{ex}}^{\mathrm{B}}}{(\gamma^{\mathrm{A}} + \gamma^{\mathrm{B}})t_{\mathrm{b}}}\left(\mathrm{e}^{-\gamma^{\mathrm{B}}|\tau|}\theta(-\tau) + \mathrm{e}^{-\gamma^{\mathrm{A}}|\tau|}\theta(\tau)\right) + \frac{N_{\mathrm{ex}}^{\mathrm{A}} N_{\mathrm{ex}}^{\mathrm{B}}}{\gamma^{\mathrm{A}}\gamma^{\mathrm{B}} t_{\mathrm{b}}^2}. \tag{S16}$$

Finally, $g_{\mathrm{AB}}^{(2)}(\tau)$ is derived as follows

$$g_{\mathrm{AB}}^{(2)}(\tau) = 1 + \frac{\gamma^{\mathrm{A}}\gamma^{\mathrm{B}}\xi^{\mathrm{AB}} t_{\mathrm{b}}}{(\gamma^{\mathrm{A}} + \gamma^{\mathrm{B}})}\left(\mathrm{e}^{-\gamma^{\mathrm{B}}|\tau|}\theta(-\tau) + \mathrm{e}^{-\gamma^{\mathrm{A}}|\tau|}\theta(\tau)\right), \tag{S17}$$

where ξ^{AB} is the excitation correlation factor and defined as

$$\xi^{\mathrm{AB}} = \lim_{N_{\mathrm{e}}\to\infty} \frac{\frac{1}{N_{\mathrm{e}}}\sum_{\mathrm{k}=1}^{N_{\mathrm{e}}} N_{\mathrm{k}}^{\mathrm{A}} N_{\mathrm{k}}^{\mathrm{B}}}{\left(\frac{1}{N_{\mathrm{e}}}\sum_{\mathrm{k}=1}^{N_{\mathrm{e}}} N_{\mathrm{k}}^{\mathrm{A}}\right)\left(\frac{1}{N_{\mathrm{e}}}\sum_{\mathrm{k}=1}^{N_{\mathrm{e}}} N_{\mathrm{k}}^{\mathrm{B}}\right)}. \tag{S18}$$

This factor theoretically equals one when the excitations of A and B are independent. Here, Eq. (S17) can be rewritten as

$$g_{\mathrm{AB}}^{(2)}(\tau) = 1 + \frac{e\xi^{\mathrm{AB}}}{(\tau^{\mathrm{A}} + \tau^{\mathrm{B}})I_{\mathrm{b}}}\left[\mathrm{e}^{-|\tau|/\tau^{\mathrm{B}}}\theta(-\tau) + \mathrm{e}^{-|\tau|/\tau^{\mathrm{A}}}\theta(\tau)\right], \tag{S19}$$

where $\tau^{\mathrm{A(B)}}$ is the lifetime of the A(B) and defined as $\gamma^{\mathrm{A(B)}} = 1/\tau^{\mathrm{A(B)}}$. In the main text, A and B are substituted to e (electron) and p (photon).

It is worth noting the difference between the 2nd order cross-correlation function $g^{(2)}_{\mathrm{AB}}(\tau)$ and the 2nd order autocorrelation function $g^{(2)}_{\mathrm{A(auto)}}(\tau)$ in the conventional HBT experiment. Considering the two materials A and B to be identical, Eq. (S19) provides the 2nd order cross-correlation function of the emission from the same sample $g^{(2)}_{\mathrm{AA}}(\tau)$. When the two materials are excited independently, $g^{(2)}_{\mathrm{AA}}(\tau)$ does not equal to $g^{(2)}_{\mathrm{A(auto)}}(\tau)$. The autocorrelation function $g^{(2)}_{\mathrm{A(auto)}}(\tau)$ is described by assuming that the same number of emitters are excited by each incident electron in both materials A and B. This assumption implies that $N^{\mathrm{A}}_{\mathrm{k}} = N^{\mathrm{B}}_{\mathrm{k}}$ in Eq. (S18). To derive the 2nd order autocorrelation function $g^{(2)}_{\mathrm{A(auto)}}(\tau)$, the parameter ξ^{AB} should be replaced by the excitation autocorrelation factor $\xi^{\mathrm{A}}_{\mathrm{auto}}$, which is described as

$$\xi^{\mathrm{A}}_{\mathrm{auto}} = \lim_{N_{\mathrm{e}}\to\infty} \frac{\frac{1}{N_{\mathrm{e}}}\sum_{\mathrm{k}=1}^{N_{\mathrm{e}}}\left(N^{\mathrm{A}}_{\mathrm{k}}\right)^2}{\left(\frac{1}{N_{\mathrm{e}}}\sum_{\mathrm{k}=1}^{N_{\mathrm{e}}} N^{\mathrm{A}}_{\mathrm{k}}\right)^2}. \tag{S20}$$

To see the relationship to the previously derived formula of the autocorrelation function[2], we now introduce an ensemble $\{N^{\mathrm{Ae}}_{\mathrm{l}}\}^{N^{\mathrm{A}}}_{l=1}$, a subset of $\{N^{\mathrm{A}}_{\mathrm{k}}\}^{N_{\mathrm{e}}}_{\mathrm{k}=1}$ composed only of the actually excited events ($N^{\mathrm{A}}_{\mathrm{k}} \geq 1$). The number of the element of the $\{N^{\mathrm{Ae}}_{\mathrm{l}}\}^{N^{\mathrm{A}}}_{l=1}$ is described as $N^{\mathrm{A}} = \eta^{\mathrm{A}} N_{\mathrm{e}}$, where η^{A} is the excitation probability. Using $N^{\mathrm{Ae}}_{\mathrm{l}}$ and $N^{\mathrm{A}} = \eta^{\mathrm{A}} N_{\mathrm{e}}$, Eq. (S20) is rewritten as below.

$$\xi_{\mathrm{auto}}^{\mathrm{A}} = \lim_{N_{\mathrm{e}}\to\infty} \frac{N_e}{N^{\mathrm{A}}} \frac{\frac{1}{N^{\mathrm{A}}}\sum_{\mathrm{l}=1}^{N^{\mathrm{A}}}\left(N_{\mathrm{l}}^{\mathrm{Ae}}\right)^2}{\left(\frac{1}{N^{\mathrm{A}}}\sum_{\mathrm{l}=1}^{N^{\mathrm{A}}} N_{\mathrm{l}}^{\mathrm{Ae}}\right)^2} = \frac{1}{\eta^{\mathrm{A}}} \lim_{N_{\mathrm{e}}\to\infty} \frac{\frac{1}{N^{\mathrm{A}}}\sum_{\mathrm{l}=1}^{N^{\mathrm{A}}}\left(N_{\mathrm{l}}^{\mathrm{Ae}}\right)^2}{\left(\frac{1}{N^{\mathrm{A}}}\sum_{\mathrm{l}=1}^{N^{\mathrm{A}}} N_{\mathrm{l}}^{\mathrm{Ae}}\right)^2} \quad \text{(S21)}$$

This is the form of the excitation autocorrelation factor, which is proportional to $\frac{1}{\eta^{\mathrm{A}}}$. Inserting Eq. (S21) to Eq. (S19), we obtain the autocorrelation function as

$$g_{\mathrm{A(auto)}}^{(2)}(\tau) = \frac{e\xi_{\mathrm{auto}}^{\mathrm{A}}}{2\tau^{\mathrm{A}} I_{\mathrm{b}}} e^{-\frac{|\tau|}{\tau^{\mathrm{A}}}} + 1, \quad \text{(S22)}$$

which is in agreement with the autocorrelation function derived in the previous study[2].

Supplementary Note 2:

PHOTON-PHOTON CORRELATION FUNCTION OF THE SCINTILLATORS

We used bulk Y_2SiO_5:Ce (YSO) and polyvinyl toluene-based plastic scintillators for the electron detectors. Here, the correlation curves of these two materials were measured by the conventional HBT measurements of CL and are shown in Fig. S2. The measurements were performed under the same conditions as described in the main text, i.e., accelerating voltage 80kV, electron beam current 4.8 pA and at room temperature. The lifetimes are $\tau^{\mathrm{YSO}} = 50.5 \pm 0.1$ ns and $\tau^{\mathrm{plastic}} = 2.89 \pm 0.08$ ns, and these are in good agreement with previously reported values[3] and catalog specifications.

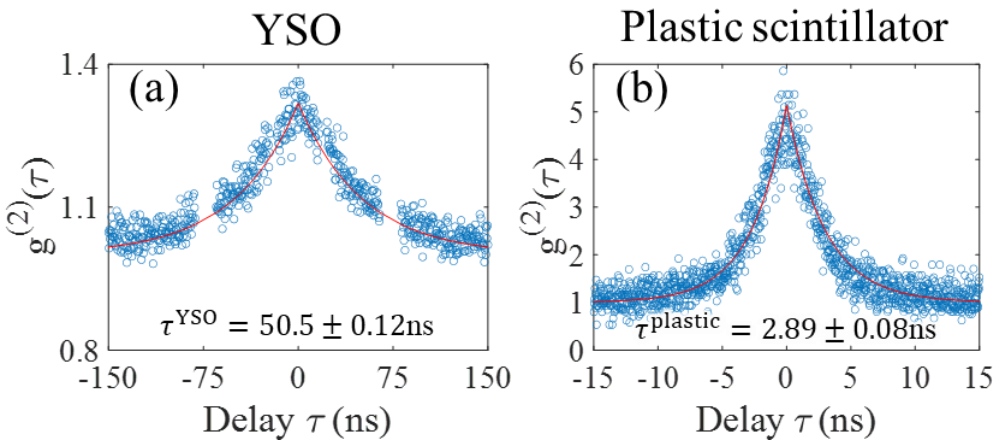

Fig. S2 Photon-photon correlation functions for the two scintillators. (a) and (b) show the correlation curves of YSO and plastic scintillators, respectively. In the YSO plot, the data missing around $\pm$75 ns is caused by removing the noise due to the reflections at the end of the optical fibers, which are used for sending photons into SPCMs.

Supplementary Note 3:

MEASUREMENT AREA OF NANODIAMOND SAMPLES

In the measurement using the YSO and Plastic scintillators in Fig. 2 in the main text, the electron beam is scanned over the area of the nanodiamond particle (NDP) sample, as shown in the red rectangle in Fig. S3. The electron beam current is set at 4.8 pA for both measurements.

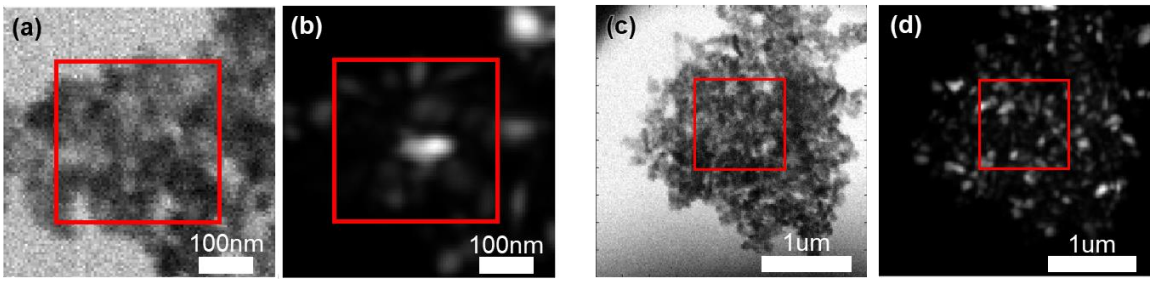

Fig. S3 Images of the samples. (a, b) and (c, d) are images of nanodiamond particle (NDP) samples used in measurements with YSO and Plastic scintillators, respectively. (a, c) STEM bright-field images. (b, d) Panchromatic CL images of NDP samples. The red rectangles indicate the electron beam scan areas for the correlation measurement.

Supplementary Note 4:

DECAY FACTOR p_{ss} DUE TO BACKGROUND NOISE

In electron-photon correlation measurements, background noise such as dark counts of the detectors and ambient stray light decrease the $g^{(2)}_{\mathrm{AB}}(0)$ value and the excitation correlation factor ξ^{AB}. Here, we consider the effect of such noises on the 2nd order cross-correlation function. The CL intensities of the material A and B with the noise are defined as

$$I^{\mathrm{A(B)}}(t) = I_{\mathrm{s}}^{\mathrm{A(B)}}(t) + I_{\mathrm{n}}^{\mathrm{A(B)}}, \tag{S23}$$

where $I_{\mathrm{s}}^{\mathrm{A(B)}}(t)$ and $I_{\mathrm{n}}^{\mathrm{A(B)}}$ indicate the intensity of the signal and the noise, respectively. Using Eq. (S23), the cross-correlation function considering the noise effect $g^{(2)}_{\mathrm{AB(noise)}}(\tau)$ is calculated as

$$g^{(2)}_{\mathrm{AB(noise)}}(\tau) = \frac{\langle I^{\mathrm{A}}(t+\tau)I^{\mathrm{B}}(t)\rangle}{\langle I^{\mathrm{A}}(t+\tau)\rangle\langle I^{\mathrm{B}}(t)\rangle} = \frac{\langle I_{\mathrm{s}}^{\mathrm{A}}(t+\tau)I_{\mathrm{s}}^{\mathrm{B}}(t)\rangle + \langle I_{\mathrm{s}}^{\mathrm{A}}(t+\tau)I_{\mathrm{n}}^{\mathrm{B}}\rangle + \langle I_{\mathrm{n}}^{\mathrm{A}}I_{\mathrm{s}}^{\mathrm{B}}(t)\rangle + \langle I_{\mathrm{n}}^{\mathrm{A}}I_{\mathrm{n}}^{\mathrm{B}}\rangle}{(\langle I_{\mathrm{s}}^{\mathrm{A}}(t)\rangle + \langle I_{\mathrm{n}}^{\mathrm{A}}\rangle)(\langle I_{\mathrm{s}}^{\mathrm{B}}(t)\rangle + \langle I_{\mathrm{n}}^{\mathrm{B}}\rangle)}. \tag{S24}$$

Since the signal and noise have no temporal relation and are uncorrelated, the following equation holds:

$$\frac{\langle I_{\mathrm{s}}^{\mathrm{A}}(t+\tau)I_{\mathrm{n}}^{\mathrm{B}}\rangle}{\langle I_{\mathrm{s}}^{\mathrm{A}}(t+\tau)\rangle\langle I_{\mathrm{n}}^{\mathrm{B}}\rangle} = \frac{\langle I_{\mathrm{n}}^{\mathrm{A}}I_{\mathrm{s}}^{\mathrm{B}}(t)\rangle}{\langle I_{\mathrm{n}}^{\mathrm{A}}\rangle\langle I_{\mathrm{s}}^{\mathrm{B}}(t)\rangle} = \frac{\langle I_{\mathrm{n}}^{\mathrm{A}}I_{\mathrm{n}}^{\mathrm{B}}\rangle}{\langle I_{\mathrm{n}}^{\mathrm{A}}\rangle\langle I_{\mathrm{n}}^{\mathrm{B}}(t)\rangle} = 1. \tag{S25}$$

Using Eq. (S24) and (S24), $g_{\mathrm{AB(noise)}}^{(2)}(\tau)$ is given by

$$g_{\mathrm{AB(noise)}}^{(2)}(\tau) = \frac{ep_{\mathrm{ss}}\xi^{\mathrm{AB}}}{(\tau^{\mathrm{A}}+\tau^{\mathrm{B}})I_{\mathrm{b}}}\left[\mathrm{e}^{-|\tau|/\tau^{\mathrm{B}}}\theta(-\tau) + \mathrm{e}^{-|\tau|/\tau^{\mathrm{A}}}\theta(\tau)\right] + 1. \tag{S26}$$

Here, p_{ss} is the decay factor and defined as

$$p_{\mathrm{ss}} = \frac{\langle I_{\mathrm{s}}^{\mathrm{A}}(t+\tau)\rangle\langle I_{\mathrm{s}}^{\mathrm{B}}(t)\rangle}{(\langle I_{\mathrm{s}}^{\mathrm{A}}(t)\rangle + \langle I_{\mathrm{n}}^{\mathrm{A}}\rangle)(\langle I_{\mathrm{s}}^{\mathrm{B}}(t)\rangle + \langle I_{\mathrm{n}}^{\mathrm{B}}\rangle)}. \tag{S27}$$

The decay factor p_{ss} is obviously less than one, and Eq. (S26) indicates that the experimentally obtained bunching height $g_{\mathrm{AB(noise)}}^{(2)}(0)$ decreases from the original value by p_{ss}. When the noise intensity $\langle I_{\mathrm{n}}^{\mathrm{A(B)}}\rangle$ is much smaller than the signal intensity $\langle I_{\mathrm{s}}^{\mathrm{A(B)}}(t)\rangle$, $p_{\mathrm{ss}} \cong 1$ holds and Eq. (S26) equals to Eq. (S19). However, if the sample is too thick for the fast electrons to transmit, the intensity of the scintillator $\langle I_{\mathrm{s}}^{\mathrm{B}}(t)\rangle$ becomes as weak as the noise intensity. Alternatively, if the photon intensity from the sample is very weak, *e.g.* for too thin samples or without presence of the sample, $\langle I_{\mathrm{s}}^{\mathrm{A}}(t)\rangle$ may also be small compared to the noise signal. In such cases, Eq. (S27) shows that p_{ss} becomes lower than one and reduces the $g_{\mathrm{AB(noise)}}^{(2)}(0)$.

Supplementary Note 5:

CL SPECTRA OF THE SAMPLES

CL spectra of nanodiamond particles (NDPs), gold nanoparticles (AuNPs) and $CsPbBr_3$ (CPB) are shown in Fig. S4. From the spectrum of the AuNP sample, one can confirm that the emission is dominantly from the coherent surface plasmons with negligible contribution from the inter-band transition .

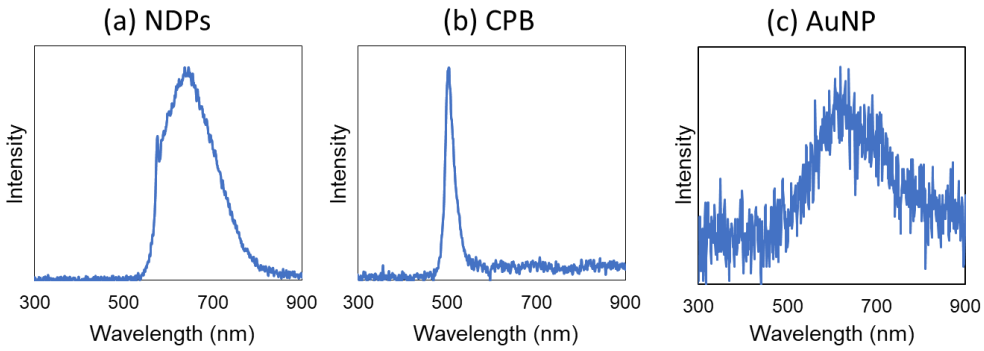

Fig. S4 CL spectra of (a) NDPs, (b) CPB and (c) AuNP.

Supplementary Note 6:

$g_{AB}^{(2)}(\tau)$ FOR COHERENT CL

The derivation process of $g_{AB}^{(2)}(\tau)$ in Eq. (19) is based on the assumption that both materials A and B show incoherent CL. Here, we consider a sample A exhibiting coherent CL, *e.g.,* Au nanoparticle. The temporal evolution of the electric field, which is coherently excited by a fast electron, has been

theoretically described in previous studies[4]. According to the temporal profile of the field, we can reasonably assume that the amplitude of the electric field rises promptly and decays exponentially. In the condition that the beam current is sufficiently small with negligible overlaps of the excitation events, the emission intensity $I^{\mathrm{A}}(t)$ can be described as

$$I^{\mathrm{A}}(t) \propto |E^{\mathrm{A}}(t)|^2 = \sum_{\mathrm{k}=1}^{N_{\mathrm{e}}} M_{\mathrm{k}}^{\mathrm{A}} e^{-2\gamma^{\mathrm{A}}(t-t_{\mathrm{k}})}\, \theta(t-t_{\mathrm{k}}). \tag{S28}$$

$M_{\mathrm{k}}^{\mathrm{A}}$ is a dimensionless coefficient, defined as $M_{\mathrm{k}}^{\mathrm{A}} = 1$ when the excitation takes place and otherwise $M_{\mathrm{k}}^{\mathrm{A}} = 0$. The mean value of $M_{\mathrm{k}}^{\mathrm{A}}$ for the whole electron incident events corresponds to the excitation efficiency. Since Eq. (S7) and Eq. (S28) are identical, we can deduce an equivalent form of ξ^{AB} as Eq. (S18) also for coherent CL.

Supplementary Note 7:

INSTRUMENT RESPONSE FUNCTION

The correlation function is obtained as the convolution of the curves reflecting the physical properties of the sample and the instrument response function (IRF). Therefore, it is necessary to consider the IRF, especially for short-lifetime material. Our experimental setup for correlation measurement consists of two single-photon counting modules (SPCMs) (PDM, MPD, Italy) and the correlation electronics (TimeHarp260 PICO, Pico Quant, Germany). By performing HBT

measurement of ultrafast pulsed laser, IRF for our system is extracted. The pulse width is 50 fs, which is four orders magnitude smaller than the specification response time of each instrument. Therefore, we can obtain IRF through this measurement.

Figure S5 shows results with the ultrafast pulse laser at two wavelengths, 400 and 800 nm. By fitting with the following equation

$$g^{(2)}(\tau) = a_1 \exp\left(-\frac{|\tau|}{\tau^1}\right) + a_2 \exp\left(-\frac{|\tau|}{\tau^2}\right) + 1, \tag{S29}$$

two overlapping exponential curves with decay times of about 52 ps and 350 ps were obtained for both wavelengths, as shown in Fig. S5. The wavelength dependence is small, and we estimate that the decay time of IRF is around 50~350 ps.

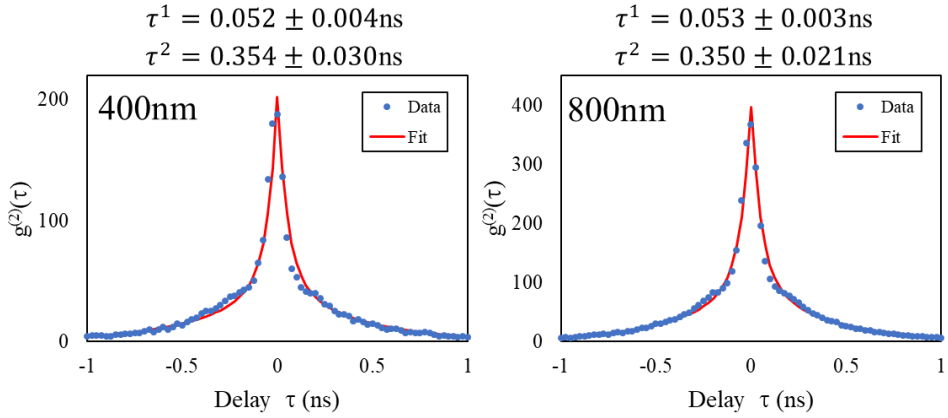

Fig. S5 IRF of our set up. Correlation curves measured with a pulsed laser at two wavelengths, 400 and 800 nm. The data at the two wavelengths are fitted with two overlapping exponential curves expressed by Eq. (S29).

Supplementary Note 8:

ELECTRON OPTICS FOR MOMENTUM RESOLVED-MEASUREMENT

For the momentum- (angle-) resolved electron detection, we used TEM imaging mode, instead of STEM, without exciting the objective lens of the electron microscope. The ray-path is shown in Fig.S6. The illumination area (ca. 7 μm in diameter) as well as the parallelity of the incident electron beam is adjusted by the condenser lens set. The "diffraction" position (dashed line in the figure) is also controlled by the condenser lenses. This "diffraction" pattern is imaged on the selected area (SA) aperture plane by the objective mini lens placed below the sample. The magnification of the diffraction (or camera length) on the SA plane is dependent on the first diffraction position (dashed line). With this setup, momentum (angle) selection can be performed by the SA aperture. Using the magnification optics of the conventional TEM imaging optics, the final camera length of the diffraction on the screen can be set to up to a few hundred meters. The detection half angle is ~ 20 μrad, and the half of this detection disk is covered by the SA aperture edge for the momentum selection.

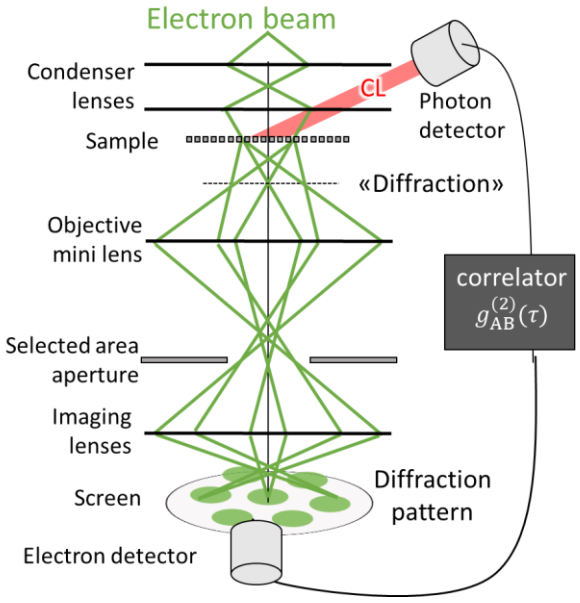

Fig. S6. Ray path of the electron beam for the electron momentum detection. The objective lens of the TEM is turned off and the electron optics is adjusted so that the "diffraction pattern" is imaged on the selected area (SA) aperture plane and (de)magnified on the screen by the magnification optics of the TEM imaging mode.

Supplementary Note 9:

PROPERTY OF CPB FOR BUILT-IN SCINTILLATOR SYSTEM

Integrating the "electron detector" scintillator into the sample substrate allows the electron-photon correlation measurement with a conventional HBT setup. We chose $CsPbBr_3$ (CPB) as the scintillator substrate, which is a perovskites semiconductor with high quantum efficiency[5]. The CL peak wavelength of CPB is around 530 nm and can be separated from that of NDP (600 nm) using an optical filter. We use two single-photon counting modules (SPCMs) (PerkinElmer, SPCM-AQR-14, USA) and correlation electronics (ORTEC, 9353, USA) for the correlation measurements of CPB. As

shown in Fig. S7, the lifetime of the CPB is $\tau^{\mathrm{CPB}} = 0.95 \pm 0.04$ ns, showing that this material works as a fast scintillator.

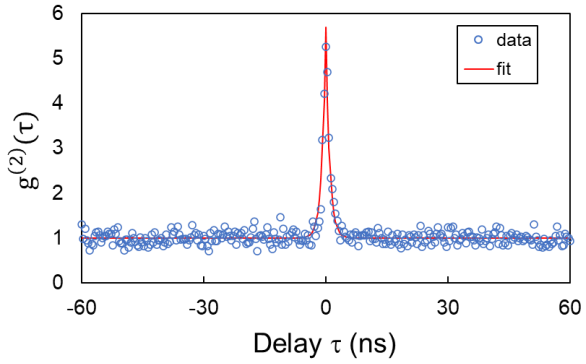

Fig. S7 Auto-correlation curve of the CPB substrate. The data is overlaid with the fitting curve shown by the red line. The obtained lifetime is $\tau^{\mathrm{CPB}} = 0.95 \pm 0.04$ ns.

Supplementary References

1. Meuret, S. *et al.* Photon bunching in cathodoluminescence. *Physical Review Letters* **114**, 1–5 (2015).
2. Yanagimoto, S., Yamamoto, N., Sannomiya, T. & Akiba, K. Purcell effect of nitrogen-vacancy centers in nanodiamond coupled to propagating and localized surface plasmons revealed by photon-correlation cathodoluminescence. *Physical Review B* **103**, 1–9 (2021).
3. Chewpraditkul, W. *et al.* Comparison of absorption, luminescence and scintillation characteristics in Lu1.95Y0.05SiO5:Ce,Ca and Y 2SiO5:Ce scintillators. *Optical Materials* **35**, 1679–1684 (2013).
4. Brenny, B. J. M., Polman, A. & García De Abajo, F. J. Femtosecond plasmon and photon wave packets excited by a high-energy electron on a metal or dielectric surface. *Physical Review B* **94**, 1–11 (2016).
5. Lin, K. *et al.* Perovskite light-emitting diodes with external quantum efficiency exceeding 20 per cent. *Nature* **562**, 245–248 (2018).